The Development of a Novel Single-pan Scanning Calorimeter and Its Use for the Measurement of Thermophysical Properties[1]

H. B. Dong[2,3] and J. D.Hunt[2]

---

[1] Paper presented at the Fourteen Symposium on Thermophysical Properties, June 25-30, 2000, Boulder, Colorado, U.S.A

[2] Department of Materials, University of Oxford, Parks Road, Oxford, OX1 3PH, U.K.

[3] To whom correspondence should be addressed

ABSTRACT

In this paper problems associated with a conventional heat-flux DSC are discussed. It is pointed out that the existence of a reference pan and a large thermal resistance between the sample and sample thermocouple cause significant measurement errors.

A single pan calorimeter has been designed and built which can eliminate the errors found in a conventional two pan DSC. A series of experiments have been carried out on pure metals and alloys to investigate reproducibility, accuracy and temperature resolution in the single-pan calorimeter, and the results are reported. It was found that enthalpy changes and heat capacity were repeatable to within 1%. The apparent latent heat and heat capacity did not depend on specimen size or significantly on rate of heating as occurs in a two-pan DSC. During the melting of pure Al, more than 80% of the latent heat was evolved over a temperature of 0.04 K. In alloys, separate heat capacity peaks for different reaction less than 1 K apart can be resolved.

It is concluded that the reference pan in a traditional heat flux DSC serves no real purpose and leads to measurement errors that are difficult to eliminate. The new single pan calorimeter allows accurate enthalpy measurements to be made with an extremely good temperature resolution.

KEY WORD: alloy, calorimetry, enthalpy change, heat capacity, heat flux DSC, metals, temperature measurement

1. INTRODUCTION

Differential scanning calorimetry (DSC) is used to measure thermal properties as a function of temperature or to measure the onset of phase transformations. Traditionally the heat-flux DSC is used at high temperatures and consists of a reference pan and a sample pan contained in a constant temperature enclosure. See figure 1a. Typically the enclosure temperature is increased or decreased at a constant rate. The lag in temperature of the reference and sample represent a heat flux to or from the surroundings.

In figure 2a, the enclosure temperature T_F, reference temperature T_R and sample temperature T_S are plotted schematically against time. As the enclosure temperature rises at a constant rate, the sample and reference temperature soon rise at the same rate; when the pure metal sample begins to melt, T_S remains constant until the sample is completely melted. When melted, T_S rises rapidly and again eventually reaches a steady state difference. The temperature differences $\Delta T_{FS} = T_F - T_S$ and $\Delta T_{FR} = T_F - T_R$ are plotted against time t, in figure 2b. Assuming heat fluxes are proportional to the temperature difference between the sample and the surroundings means that the product of the temperature difference and time is proportional to the enthalpy change. The hatched areas in figure 2b are proportional to the enthalpy changes from t_1 to t_2 in the sample and reference.. The difference in temperature between the sample and reference $\Delta T_{RS} = T_R - T_S$ thus gives a measure of the difference in enthalpy change of the sample and reference over the time interval. A calibrant of known enthalpy as a function of temperature allows absolute enthalpy changes to be calculated.

It is often assumed that the difference ΔT_{RS} is proportional to the difference in heat capacity between the sample and reference. This is true when the sample and

reference temperature change at the same rate, but is not true when the changes are different. This is apparent from figure 2c where the temperature differences are plotted against temperature. Immediately after melting ΔT_{RS} is large because the sample temperature is rising more rapidly than the reference. Neglect of this effect leads to smearing of the temperature over which latent heat is apparently evolved [1]. If effective heat capacity (heat capacity plus latent heat) is to be measured as a function of temperature, great care must be taken to ensure that the de-smearing calculations are rigorous [2]. Although the difference in enthalpy of the reference and sample between time t_1 and t_2 is defined in fig 1b, the temperature change in the sample and reference are very different.

Other problems arise with a heat-flux DSC. When large heat fluxes are present the thermocouples do not measure the temperature of the sample or reference. This is because the thermal resistance between the sample (or reference) and its thermocouple is significant when compared with the thermal resistance between the thermocouple and the surroundings. To a first approximation the two temperature drops might be expected to be proportional to one another. This would result in a sample thermocouple temperature T_T, plot against time similar to that shown by the dashed line in figure 2a. The plot of apparent temperature differences would appear as the dashed line in figure 2c. The important feature is that even though the sample melts at one temperature heat appears to be absorbed over a range of temperatures. Some experimental result was discussed in section of result and discussion.

Another potentially serious problem for measuring real changes in enthalpy is that for large temperature differences between sample and reference, heat flows from the reference to the sample (or vice versa) thus giving erroneous enthalpy changes.

These three effects explain why it is generally recognised that small samples must be used in a two-pan calorimeter when a significant amount of latent heat is evolved. The problem is deciding how small the sample should be for accurate results.

It is difficult to see the reason for using a reference pan. The difference in temperature between the sample and the enclosure contains similar information to that of the temperature difference between sample and reference (see figure 2b). In addition the absence of a reference pan means the heat flow within the enclosure is geometrically simple and can be easily analysed. These considerations led to the development of a simple single-pan calorimeter that appears to eliminate many of the problems in a conventional heat-flux DSC.

2. THE NEW SINGLE-PAN SCANNING CALORIMETER

The essential feature of the calorimeter is that the sample is in a uniform temperature enclosure and that it has the largest possible thermal resistance between the sample and its surroundings. A schematic diagram of the apparatus is shown in figure 1b. To ensure a uniform temperature enclosure, the outer crucible is thermally isolated from the furnace, is thick walled and made of a material with a high conductivity. The inner crucible is thermally isolated from the outer crucible to ensure the maximum temperature difference between the two crucibles. In principle there is no disadvantage in using large samples provided significant temperature differences do not arise in the sample. Sheathed 0.5 mm OD thermocouples are placed in the walls of the inner and outer crucibles. During most runs an additional thermocouple was placed in the centre of the sample. The thermocouple and a piece of thermocouple sheath act as supports for the specimen.

Computer programs have been developed to log the temperature data and to control temperature or temperature difference. The temperature of each thermocouple is sampled about 625 times a second, averaged, then stored at one-second intervals. The temperature control can operate with full PID (Proportional, Integral and Derivative) but is normally used as a PD controller. Special care has been taken to eliminate thermal drift in the pre-amplifiers and to minimise electrical noise. After properly tuning the PID parameters and power setting, the temperature of the outer crucible has typical stability of better than ±0.02 K.

The calorimeter can be operated in the normal DSC manner by changing the outer (or inner) crucible temperature at a programmed rate. Because the specimens are much larger than a conventional heat flux DSC, the calorimeter can be operated in a constant heat flux mode as was proposed by Smith 1940 [3]. In this mode the temperature difference between the sample and the surroundings is kept constant. This means the temperature rises less rapidly when latent heat is absorbed. Figure 3 a, b and c show temperature and temperature difference plotted against time for pure Al and illustrate the different operational modes. In figure 3a the outer temperature was increased at a constant rate; in figure 3b the temperature difference between the inner and outer thermocouples was kept constant (Smith mode); in figure 3c the outer crucible temperature was ramped and oscillated. Note the different behaviour in figure 3a and 3b as the metal melts.

Since the specimen is large the calorimeter is ideally suited for slow heating or cooling rates. Significant results can be obtained with heating rates as low as 0.1 K/min even so heating and cooling rates of 30 K/min have been achieved in the present apparatus.

3. ENTHALPY CALCULATION

Because of the simplicity of the single pan calorimeter, equations are easily derived to relate temperature changes to enthalpy changes. As in a conventional DSC a run is carried out with an empty pan then with the (empty pan + calibrant) and then with the (empty pan + sample). The temperature differences are first corrected with a zero line adjustment. These are measured during an isothermal anneal [1] before, during and after a run.

As the calorimeter is heated in the time interval dt the temperature of the empty inner crucible rises dT_E, the (calibrant + empty) rises dT_C and the (sample + empty) rises by dT_S. The corresponding temperature differences between the inner and outer crucible for the three cases are ΔT_{DE}, ΔT_{DC} and ΔT_{DS}. Let C_C be the change in heat content per degree (ie. heat capacity times mass) of the calibrant; this must be known as a function of temperature. Similarly C_E and C_S are those of the empty crucible and sample. It should be noted that C_S contains any latent heat and is thus an effective heat capacity. The heat transfer coefficient between the inner and outer crucible is a and is expected to be a function of temperature.

For the empty crucible $\quad a\Delta T_{DE}dt = C_E dT_E$

For the calibrant + empty $\quad a\Delta T_{DC}dt = (C_C + C_E)dT_C$

For the sample + empty $\quad a\Delta T_{DS}dt = (C_S + C_E)dT_S$

Solving these three equations gives a general expression for the rise in enthalpy of the sample dH_S in dT_S

$$C_C\left(\frac{\Delta T_{DS}-\frac{\Delta T_{DE}}{dT_E}dT_S}{\frac{\Delta T_{DC}}{dT_C}-\frac{\Delta T_{DE}}{dT_E}}\right)=C_S dT_S=dH_S \qquad (1)$$

The equation is valid as $dT_S \rightarrow 0$ and can thus handle the latent heat of a pure material. The ratios $\Delta T_{DE}/dT_E$ and $\Delta T_{DC}/dT_C$ are evaluated from the empty and calibrant + empty run at the relevant temperature using the same time interval. The meaning of these terms is best visualised by noting that the first is the inverse of $\frac{dT_E}{dt}\frac{1}{\Delta T_{DE}}$ which is the rate of rise of the empty pan divided by the difference in temperature between the inner and outer crucible. The general equation is valid for any mode of operation and that includes constant rate of temperature rise or constant heat flux. It should be emphasised that the equation and use of a central thermocouple automatically handles the de-smearing process.

4. RESULTS AND DISCUSSION

In the present work Cu has been used as the calibrant with the heat capacity data from [4]. A number of materials have been investigated using either graphite or machinable alumina for the inner crucible. In this paper, the results for pure Al, a binary Al-(0.2wt%)Fe and an Al alloy (LM25) will be reported.

4.1 Pure Al

4.1.1 Melting range of Al

Figure 4a shows the sample temperature plotted against time for melting pure Al in the new calorimeter. In these experiments the outer crucible was either heated or cooled at

a constant rate of 4 K/min. There is an initial transient of about 0.06 K, then an almost linear rise of about 0.17 K. During melting, the temperature difference between the inner and outer thermocouples changes from about 2K to 20K; the temperature difference between the inner and sample thermocouples changes from about 0.4 K to 4 K. The apparent variation in the melting temperature or the variation of the sample thermocouple temperature is about 0.23K for a 2.2 g sample (this compares with 3.7 K for the 1.36 mg sample in the two-pan DSC [1]).

Figure 4.b shows the temperature plotted against time for melting pure Al in the constant heat flux mode. In this experiment a value of 6K was used for heating and -6K for cooling. The inner crucible was alumina and the outer crucible boron nitride; this gives a heating or cooling rate in the absence of latent heat evolution of about 3.4 K/min. The temperature variation during melting and solidification is very small about 82% of the latent heat is evolved over 0.04K. About 50% of the latent heat is evolved over only 0.01 K. It can be seen on figure 5b that there is an initial transient, a plateau for about 50 % of the width, then a gradual rise in temperature and a short final transient.

4.1.2 Enthalpy change and heat capacity measurement

Enthalpy changes are calculated by using the experimental results to integrate equation 1. Figure 5a shows the enthalpy for pure Al plotted as a function of temperature. The melting and freezing lines almost coincide. Figure 5b shows the effective heat capacity obtained using the slope of figure 5a for the melting line. Most of the latent heat was evolved over a temperature change of only 0.04 K. The important feature is the narrowness of the effective heat capacity peak. It is not possible to get

such a narrow peak with a conventional heat-flux DSC for the reasons discussed in the introduction. Very good reproducibility can be obtained. The average values and standard deviation for seven runs for heat capacity and latent heat are compared with [4] in Table 1. The table also shows runs carried out with different heat fluxes. Less than 1% variation is obtained between samples and runs using the same sample.

4.2 Binary (Al – 0.2wt%Fe)

Figure 6 a and b show the enthalpy change and heat capacity of Al-0.2wt%Fe plotted as a function of temperature with the constant heat flux mode. Again the melting and freezing enthalpy lines almost coincide except for the supercooling before the aluminium dendrite and eutectic nucleates. The average and standard deviation of six runs results, for the non-equilibrium solidus, non-equilibrium liquidus, heat capacity and latent heat are given in Table2

4.3 Alloy LM25 (Al – 7.3wt%Si, 0.37wt%Fe, 0.16wt%Mn, 0.46wt%Mg, 0.07wt%Cu)

Figure 7 a-c shows the enthalpy change and effective heat capacity for LM25 measured using the constant heat-flux mode. The enthalpy line is different for melting and freezing (see figure 7a) and this is consistent with a departure from equilibrium as freezing takes place. The effective heat capacity for melting, figure 7b, and for freezing, figure 7c, shows a number of transitions. On freezing Al dendrite is formed at about 620 ^{o}C and continues to be deposited until a eutectic (Al+Si) comes out at about 570 ^{o}C; finally a ternary eutectic (Al+Si+β) is deposited at about 550 ^{o}C. On heating the lowest temperature peak splits into two separated by about 2 K. It is possible that the additional peak is the result of a solid-state deposit of Mg_2Si. Reactions of the

ternary and solid-state deposit was not detected by [5] in a commercial heat-flux DSC , but is very apparent on all the specimens examined in the present work. The results from Electron microprobe analysis (EMPA) and XRD have confirmed the existence of the β and Mg_2Si phases. Six runs were carried out to investigate reproducibility; the results, average and standard deviation, for the solidus, liquidus, heat capacity and latent heat are given in Table 2.

5. CONCLUSION

It is concluded that the present single pan calorimeter has significant advantages over a conventional heat-flux DSC.

1) The analysis and set-up automatically removes the need for de-smearing. Similar results are obtained in pure materials at large or small heating rates or in large and small specimens.
2) High resolution is obtained for the onset of phase transformations because temperature can be measured from within a specimen.
3) Accurate heat fluxes can be measured because the heat flow path is well defined and the flux thermocouples measure temperature differences over the largest possible thermal resistance; reproducibility is better than 1%.
4) Heat flow cannot occur between a sample and a reference pan.
5) A constant heat flux mode can be used thus minimising errors due to an increasing heat flux.

ACKNOWLEDGEMENTS

The authors wish to acknowledge encouragement and helpful discussion from Dr Peter N Quested and Mike J Richardson from Centre for Materials Measurement Technology, National Physical Laboratory, Teddington, Middlesex, U.K. TW11 0LW

REFERENCES

1. G. Höhne, W.Hemmminger and H-J Flammershein, 1996, *Differential Scanning Calorimetry*, Berlin, Springer.

2. M.J. Richardson, 1992, In Compendium of Thermophysical Property Measurement Methods, New York Plenum Press, pp 519-545.

3. C.S. Smith, 1940, Trans. Amer. Inst. Met. Eng., **137** 236-245

4. R. Hultgren, P.D. Desai and D.T. Hawkins, 1973, *Selected Values of the Thermodynamic Properties of Elements.* ASM, Ohio.

5. P.N. Quested, K.C. Mills, R.F. Brookes, A.P. Day, R. Taylor and H. Szelagowski, Proceedings of the international conference on solidification processing July 1997, Sheffield University Press, pp 143-150.

Table1. Measured results on pure Al of single-pan calorimeter

	C_p at 600°C (J/K/mol)	C_p at 650°C (J/K/mol)	C_p at 670°C (J/K/mol)	L (heating) (J/mol)	L (cooling) (J/mol)
(Results for seven runs using pure Al)					
Average	31.5643	33.2529	31.40	10932	10910
Standard deviation	±0.1349	±0.1874	±0.1460	±29.31	±35.36
Hultgren et al 1973	31.52	33.14	31.72	10784±125	
(Results for pure Al using different heating/cooling rates)					
1.5	31.45	33.20	31.40	11028	10820
3.4	31.56	33.25	31.40	10932	10910
4.5	31.50	33.40	31.50	10820	10630

Table 2 Results for six runs using Al-0.2wt%Fe and LM25

	Non-equilibrium Solidus (°C)		Non-equilibrium Liquidus(°C)		Cp (J/K.mol)	Cp (J/K.mol)	Enthalpy change (J/mol)	
	heating	cooling	heating	cooling			heating	cooling
(Al-0.2wt%Fe)					(at 640°C)	(at 670°C)	(from 652°C to 659°C)	
Averaged	654.29	652.49	658.56	658.49	33.78	31.74	11152	11178
Standard deviation	±0.18	±0.21	±0.10	±0.12	±0.22	±0.06	±32.0	±41
(LM25)					(at 530°C)	(at 630°C)	(from 652°C to 659°C)	
Averaged	555.60	547.81	618.26	613.03	37.54	31.86	17551	17480
Standard deviation	±0.43	±0.63	±0.10	±0.12	±0.28	±0.074	±57.97	±56.39

Figure captions

1. (a) Schematic diagram of a conventional heat-flux DSC. (b) Schematic diagram of the calorimeter described in the present work.

2. A combined schematic plot of (a) temperature against time, (b) temperature difference against time, (c) temperature difference against temperature for a heat-flux DSC.

3. Plots of temperature of outer crucible (green lines) and temperature centre thermocouple (red lines) versus time, temperature difference versus time (dark lines) for a 2.2 g pure Al sample (a) outer crucible heated at ± 4 K/min (b) using a constant temperature difference ±3 K between sample and furnace (Smith mode), (c) outer crucible temperature ramped and oscillated.

4. Measured temperature range against time for Pure Al with single-pan calorimeter. (a) outer crucible heated at 4 K/min, (b) constant temperature difference 6K

5. Plots using pure Al for (a) enthalpy change versus temperature during melting (dark blue line) and freezing (red line), (b) effective heat capacity versus temperature for melting. Constant temperature difference 6K.

6. Plots using Al-0.2wt%Fe for (a) enthalpy change versus temperature during melting (dark blue line) and freezing (red line), (b) effective heat capacity versus temperature for melting. Constant temperature difference 6K.

7. Plots using LM25 for (a) enthalpy change versus temperature during melting (dark blue line) and freezing (red line), (b) effective heat capacity versus temperature for melting (c) effective heat capacity versus temperature for freezing. Constant temperature difference 6K.

Figure 1

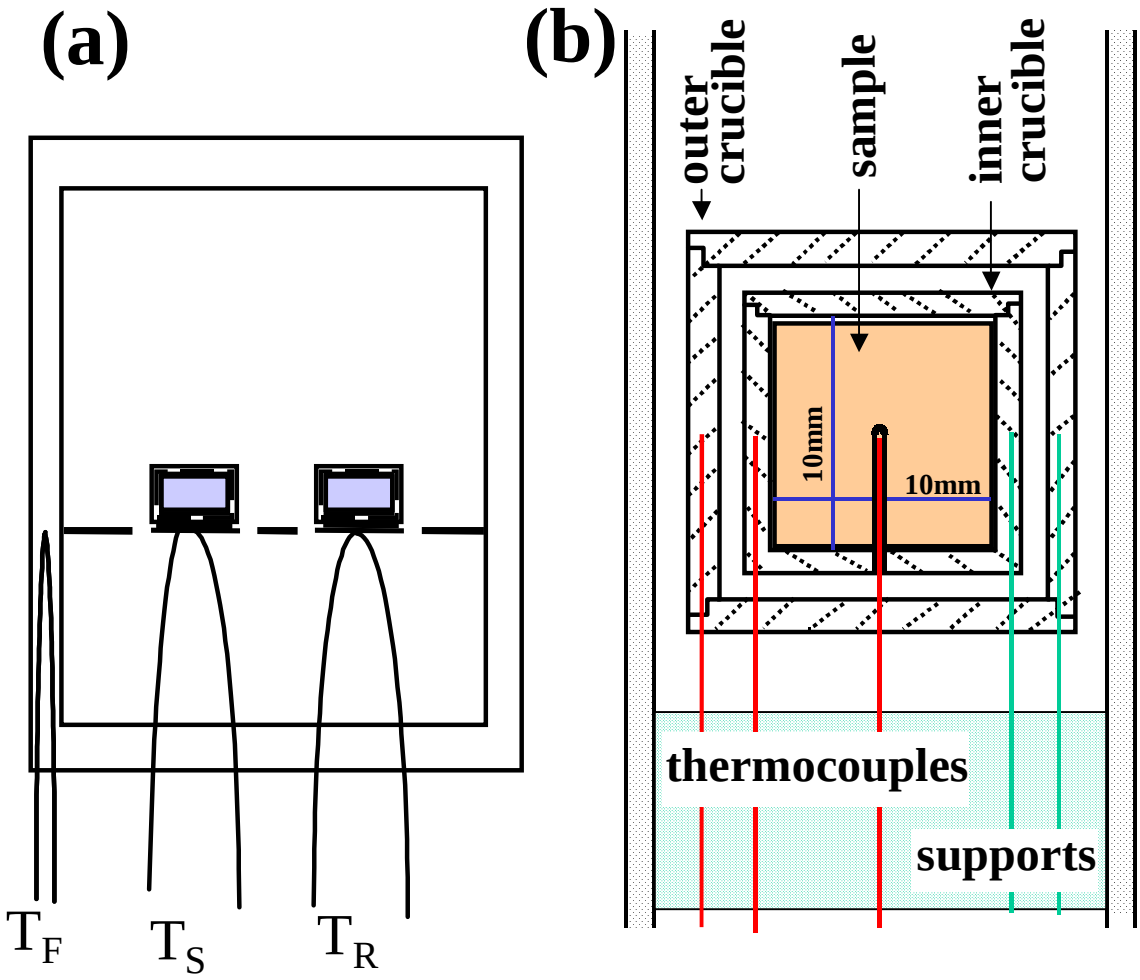
(a)
T_F
T_S
T_R
(b)
outer crucible
sample
inner crucible
10mm
10mm
thermocouples
supports

Figure 2

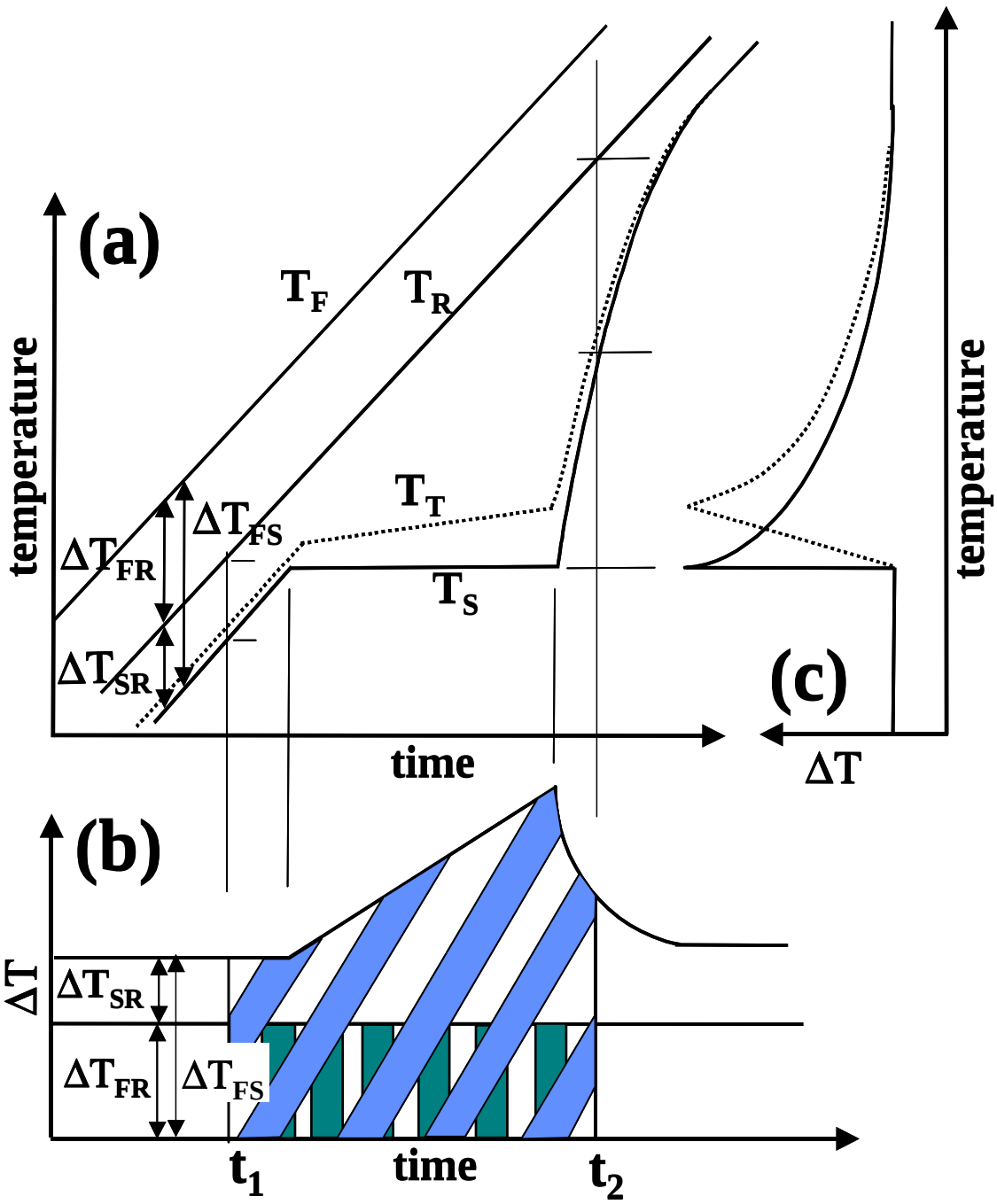
(a)
temperature
T_F
T_R
T_T
T_S
ΔT_{FS}
ΔT_{FR}
ΔT_{SR}
time
(c)
ΔT
temperature
(b)
ΔT
ΔT_{SR}
ΔT_{FR}
ΔT_{FS}
t_1
time
t_2

Figure 3

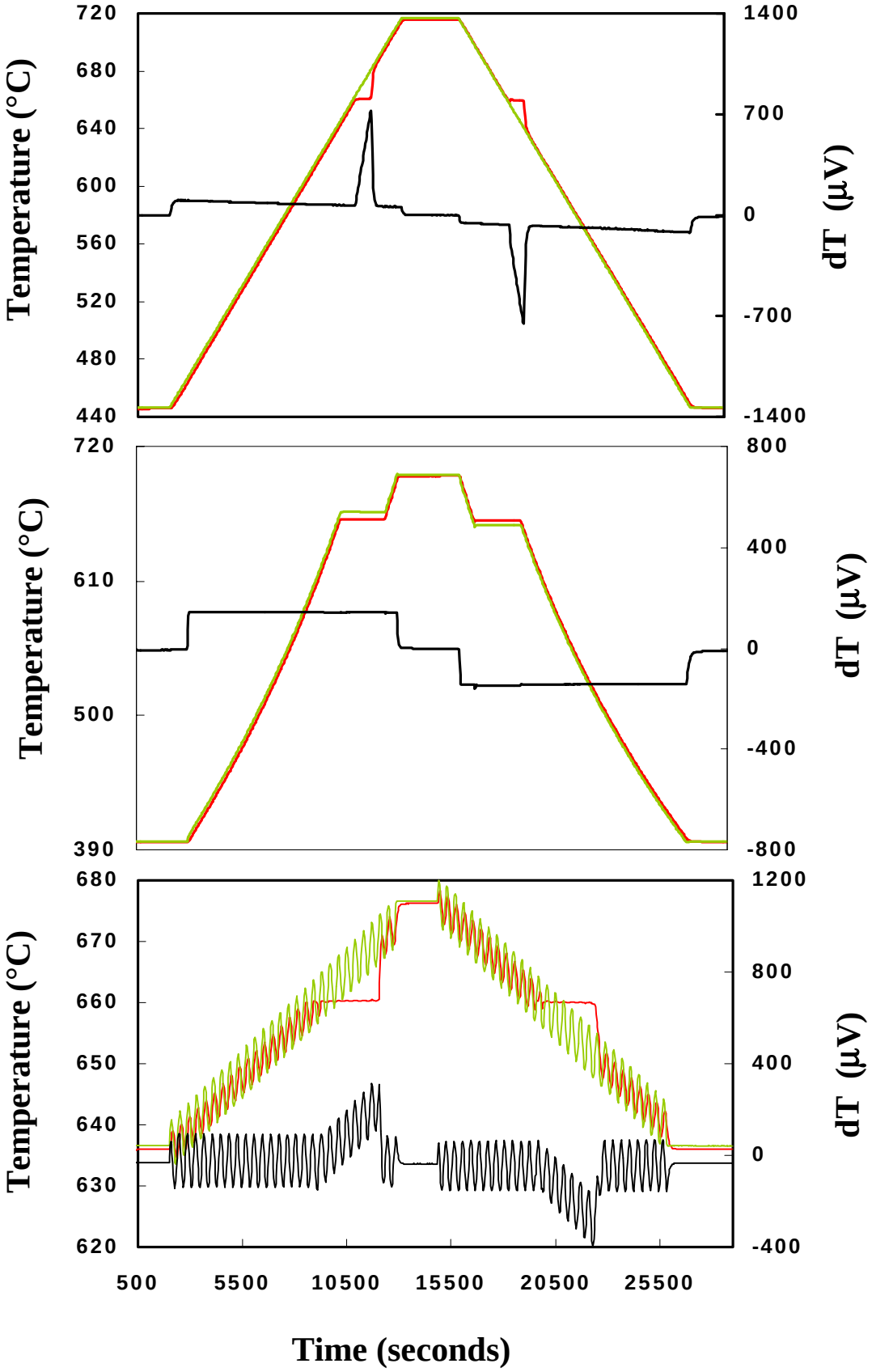
Temperature (°C)
720
680
640
600
560
520
480
440
1400
700
0
-700
-1400
dT (µV)
Temperature (°C)
720
610
500
390
800
400
0
-400
-800
dT (µV)
Temperature (°C)
680
670
660
650
640
630
620
1200
800
400
0
-400
dT (µV)
500
5500
10500
15500
20500
25500
Time (seconds)

Figure 4

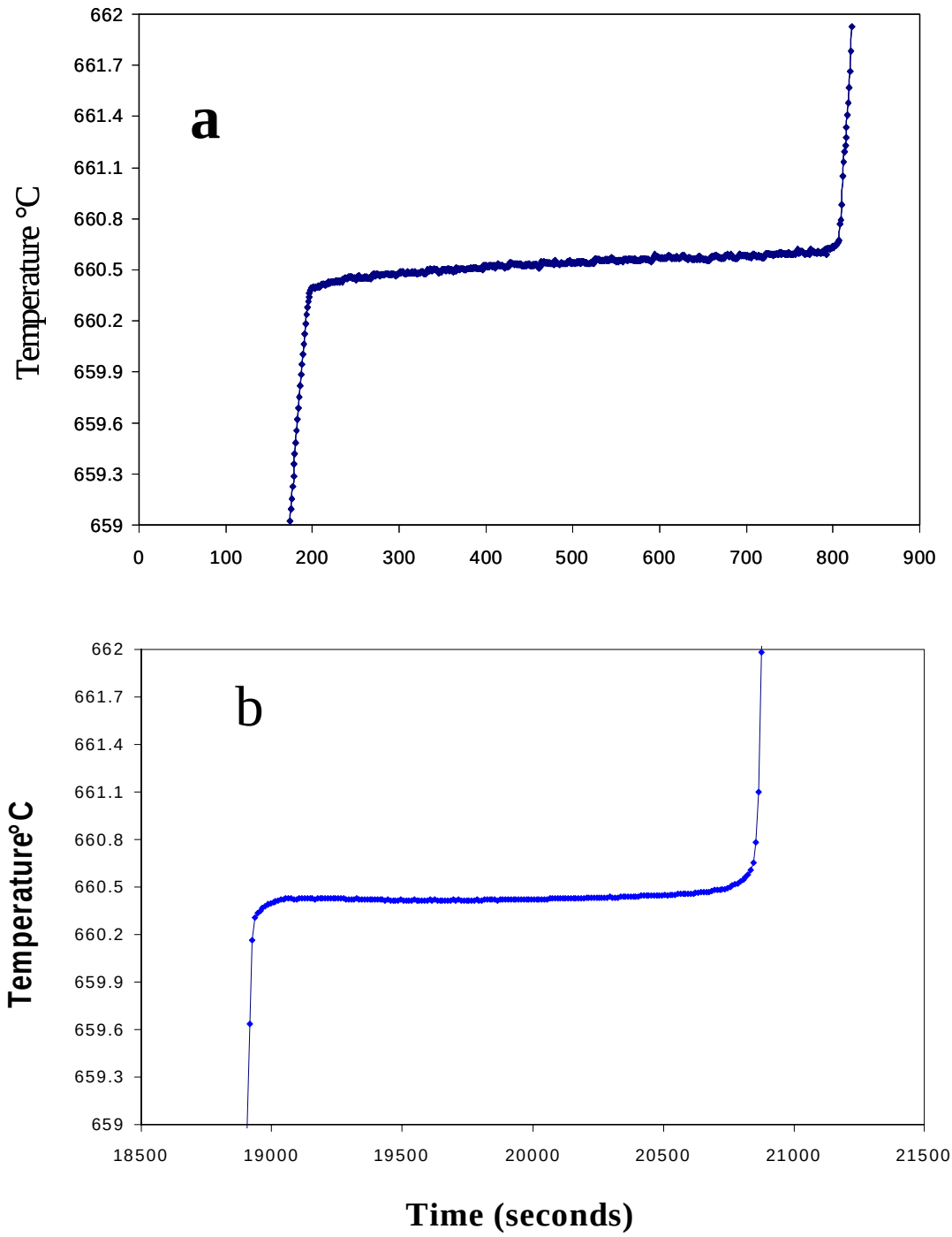
a
Temperature °C
662
661.7
661.4
661.1
660.8
660.5
660.2
659.9
659.6
659.3
659
0
100
200
300
400
500
600
700
800
900
b
Temperature°C
662
661.7
661.4
661.1
660.8
660.5
660.2
659.9
659.6
659.3
659
18500
19000
19500
20000
20500
21000
21500
Time (seconds)

Figure 5

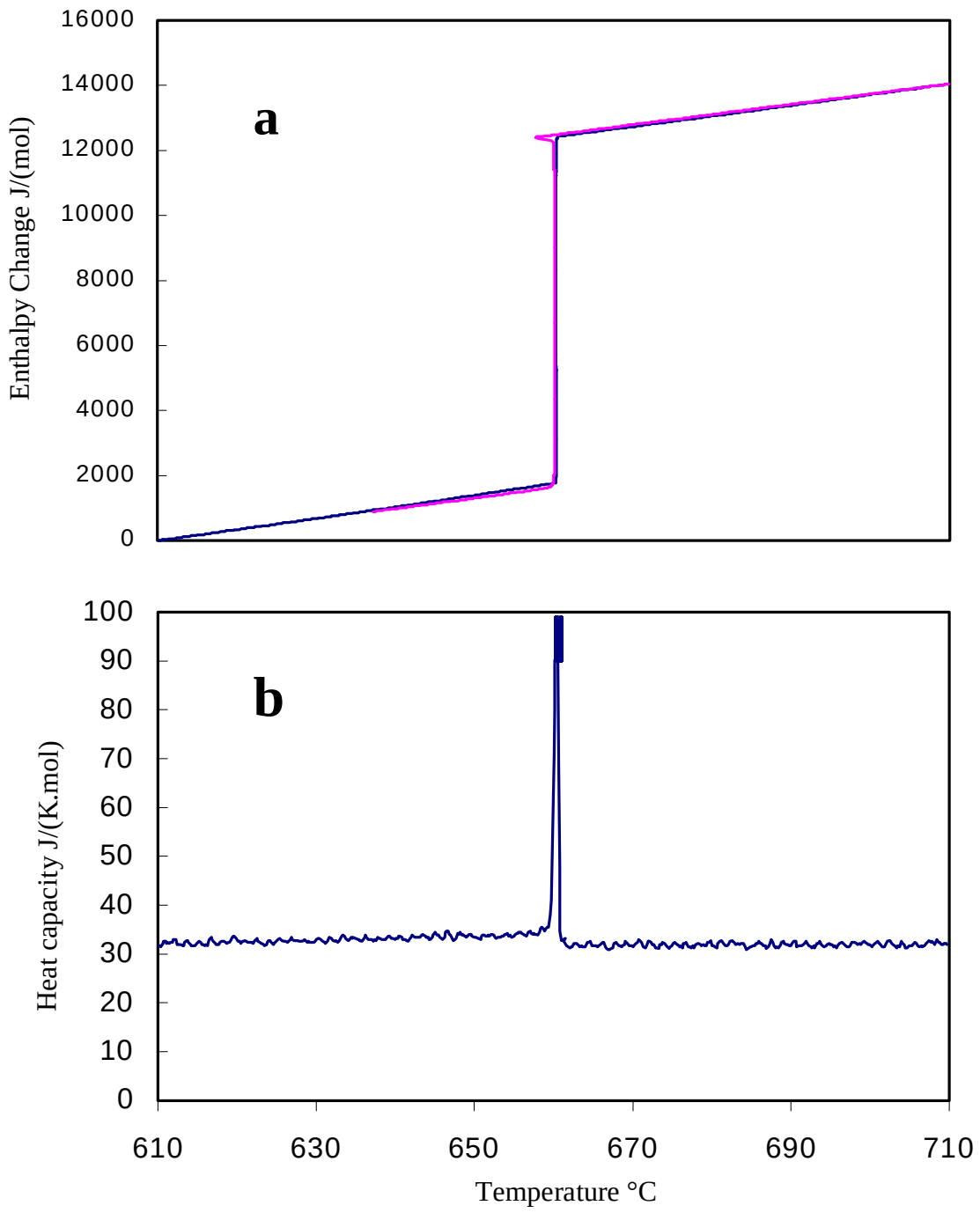
a
Enthalpy Change J/(mol)
16000
14000
12000
10000
8000
6000
4000
2000
0
b
Heat capacity J/(K.mol)
100
90
80
70
60
50
40
30
20
10
0
610
630
650
670
690
710
Temperature °C

Figure 6

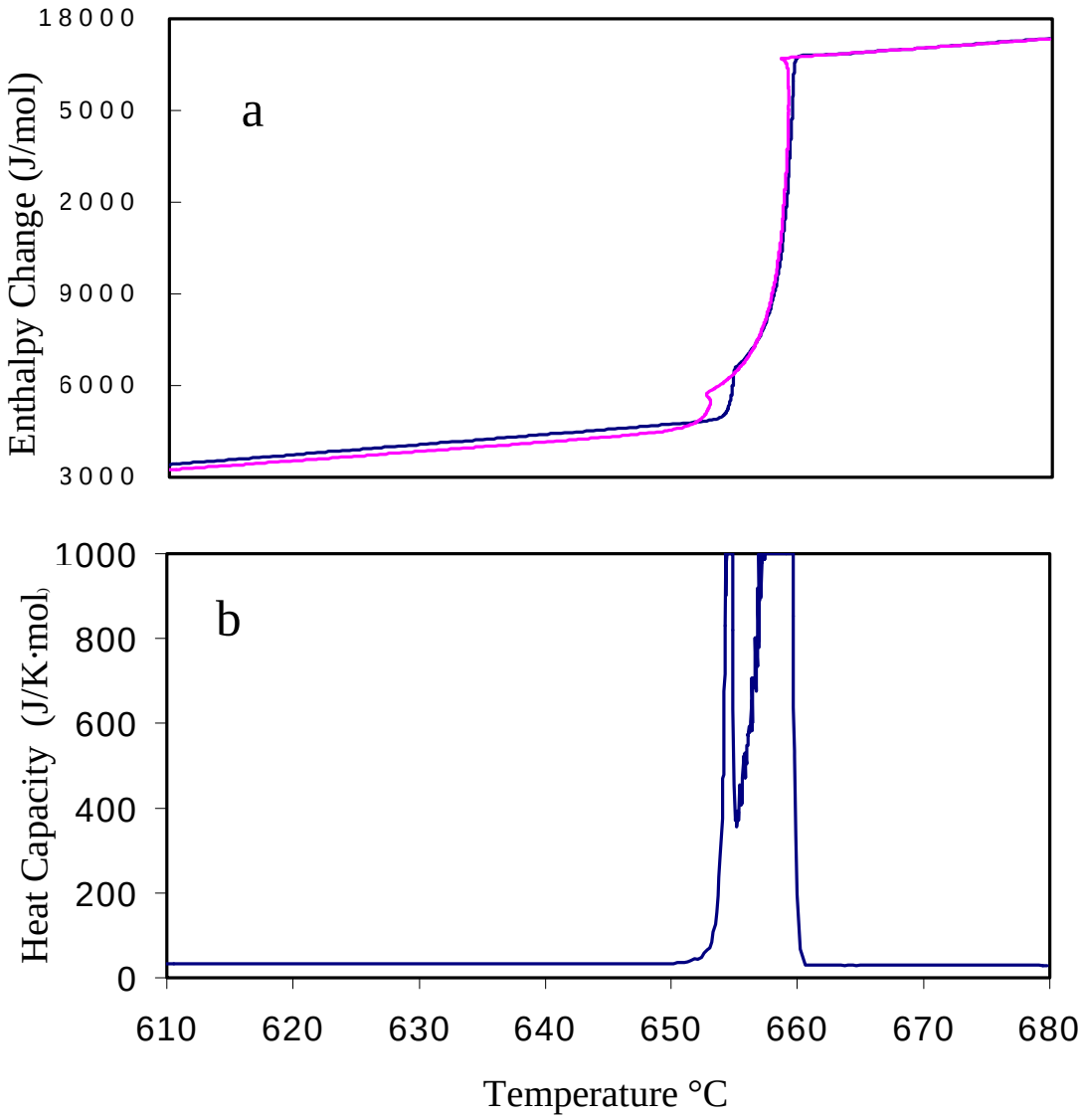
18000
5000
2000
9000
6000
3000
Enthalpy Change (J/mol)
a
1000
800
600
400
200
0
Heat Capacity (J/K·mol)
b
610
620
630
640
650
660
670
680
Temperature °C

Figure 7

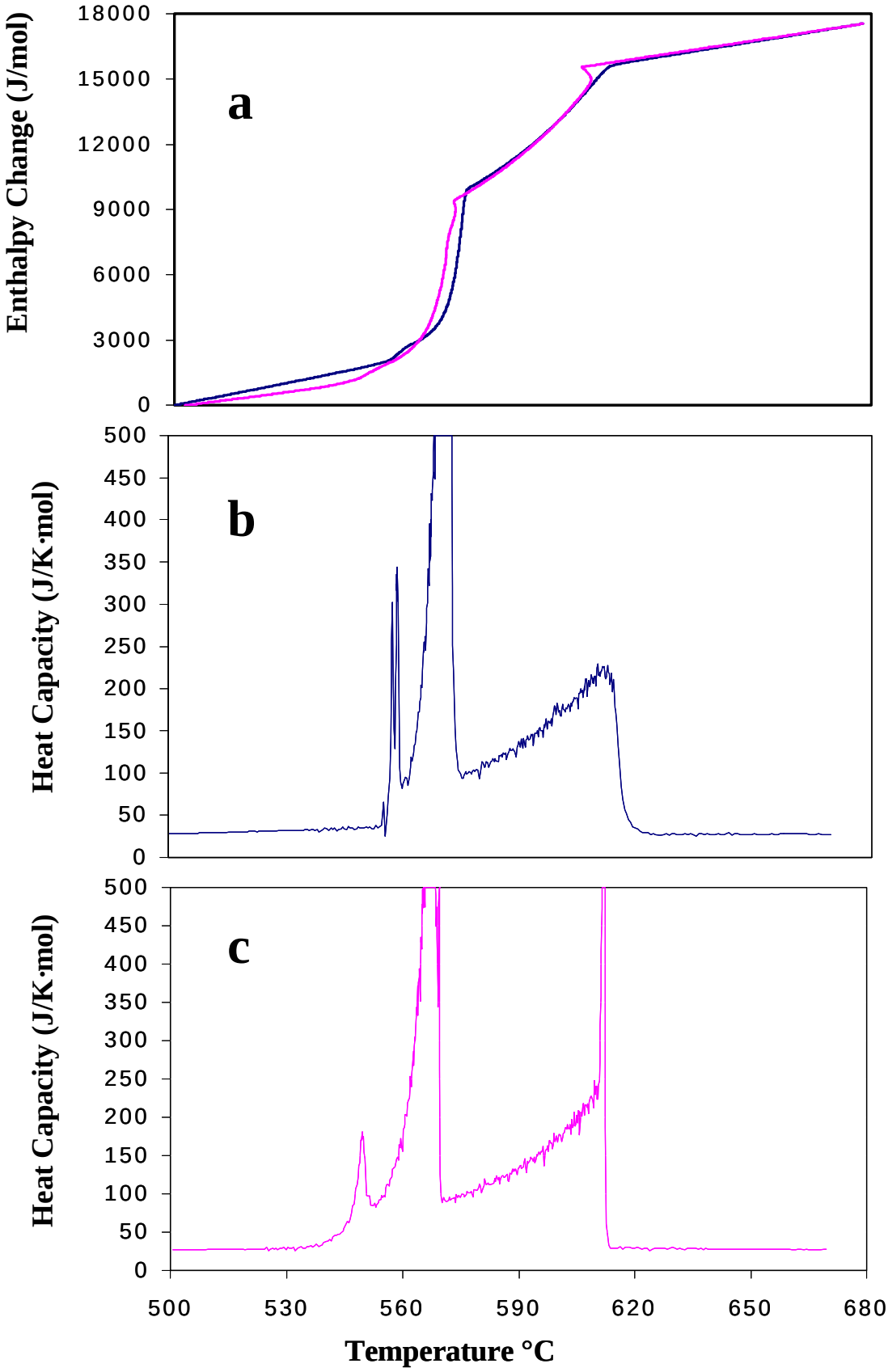
Enthalpy Change (J/mol)
18000
15000
12000
9000
6000
3000
0
a
Heat Capacity (J/K·mol)
500
450
400
350
300
250
200
150
100
50
0
b
Heat Capacity (J/K·mol)
c
500
530
560
590
620
650
680
Temperature °C